Article

Future Sensors for Smart Objects by Printing Technologies in Industry 4.0 Scenario

Michela Borghetti[ID]**, Edoardo Cantù *, Emilio Sardini**[ID] **and Mauro Serpelloni**[ID]

Department of Information Engineering, University of Brescia, Via Branze 38, 25123 Brescia, Italy; michela.borghetti@unibs.it (M.B.); emilio.sardini@unibs.it (E.S.); mauro.serpelloni@unibs.it (M.S.)
* Correspondence: e.cantu@unibs.it

check for updates

Abstract: Industry 4.0 has radically been transforming the production processes and systems with the adoption of enabling technologies, such as Internet of things (IoT), big data, additive manufacturing (AM), and cloud computing. In this context, sensors are essential to extract information about production, spare parts, equipment health, and environmental conditions necessary for improving many aspects of industrial processes (flexibility, efficiency, costs, etc.). Sensors should be placed everywhere (on machines, smart devices, objects, and tools) inside the factory to monitor in real-time physical quantities such as temperature, vibrations, deformations that could affect the production. Printed electronics (PE) offers techniques to produce unconventional sensor and systems or to make conventional objects "smart". This work aims to analyze innovative PE technologies—inkjet printing and aerosol jet printing in combination with photonic curing—as manufacturing technologies for electronics and sensors to be integrated into objects, showing a series of sensors fabricated by PE as applications that will be adopted for smart objects and Industry 4.0.

Keywords: aerosol jet printing; inkjet printing; photonic curing; flash lamp annealing; industry 4.0; I4.0; IoT; smart devices; predictive maintenance; PdM; environmental parameters monitoring

1. Introduction

In recent years, Industry 4.0 (I4.0) paradigms have started a transformation process of the traditional manufacturing systems into smart factories thanks to a series of innovations and technologies able to connect objects, machines, tools, and workers. Smart factories focus on flexibility, quality, efficiency, and predictability of the production through the adoption of enabling technologies, such as big data, Internet of things (IoT), additive manufacturing (AM), and cloud computing [1]. Big data and machine learning (ML) allow to manage a large amount of real-time data generated in the smart factory and to support decisions on the industrial processes for improving productivity; this contributes to reduced costs [1] and operator workload [2], and to speed up the decision process and improve the production [3,4].

In a smart factory, traditional machines become context-aware devices [5], and the environment is enriched with networked sensors (indoor positioning systems, cameras, etc.) to enable the interaction with operators [6]. Therefore, measuring different physical quantities (temperature, humidity, vibrations, mechanical deformations, angular velocity, etc.) that can affect the production process is essential for I4.0 to improve the quality of the final product [7] and the safety of the workers. Industrial IoT (IIoT), a network of intelligent industrial smart objects and devices, contributes to achieving a high production rate with limited operational costs and efficient control of processes, assets, and operational time through real-time monitoring [8]. A new class of devices called "smart objects" contributes to controlling not only the smart factory but also the external environment. In this scenario, traditional tools and objects involved in the industrial processes are equipped with sensors, electronics, and proper communication

protocols to sense and measure, collect and exchange data with other devices or users, who can remotely supervise the industrial systems through existing networks. For example, in [9], a safety helmet for the mining industry was made smart by the integration of off-the-shelf sensors and electronics on the helmet. The smart helmet was designed to monitor climate changes and hazardous events (temperature, humidity, gas, removal helmet of the miner) and alert the room center. Besides the advantages, bulk electronics significantly affected comfort and usage.

Maintenance, repair, and operations (MRO) of parts inventory and predictive maintenance (PdM), typical applications within I4.0, can benefit from the integration of sensors on the equipment (consumables, maintenance supplies, spare parts, and machines) involved in the process (mechanical processing, chemical plants, energy production) to predict failures. These strategies aim to reduce maintenance and repair costs, extend equipment lifecycle and guarantee worker safety with targeted actions and less waiting times. Additionally in PdM, smart objects can help to predict failure events of the machine [10]; for example, piezoelectric sensors can be successfully adopted for real-time monitoring of mechanical strength in metallic structures due to their load and strain sensing accuracy, low power consumption, and low cost [11], while strain gauges could detect tool deterioration and damage through the measurement of the mechanical stress and strain in the tool. Applicative examples can be considered in different industrial contexts, such as the oil sector [12], metallurgic industry [13], and industrial machinery [14].

The real-time monitoring of the health of machines and operators is performed by measuring different physical quantities and often requires technological advances or custom-made sensors to make tools and objects "smart", connected in real-time to the industrial network [15]. Printed electronics (PE) offers innovative technologies to make objects "smart" by fabricating new sensors and electronics according to the specific context and application. PE is also attractive for low production costs, flexibility in the design, and a high variety of materials. For example, printed sensors on flexible surfaces could be intended for harsh environments (extreme temperatures, corrosive, or hazardous substances, etc.) [16] or to be mounted on the challenging area due to the size of the components involved (turning, milling, and other mechanical tools). Furthermore, PE includes technologies able to fabricate electronics directly onto objects, without installation, assembly, or any surface modification (cleaning, scratching, gluing, etc.). This capability to manufacture fully-functioning sensors and circuits on 3D objects, without any kind of dimensional changing, will afford unprecedented scalability, miniaturization, and conformability (with great attention to materials compatibility), increasing the functionality of new products [17]. Finally, PE can be easily integrated into the process flow of additive manufacturing technologies to produce smart prototypes and objects [18]. Indeed, AM, known as 3D printing, includes promising technologies for I4.0 to quickly produce aids, functional prototypes, and even items not available on the market [19], and PE makes these products "smart" by fabricating electronics for them.

Among PE technologies, inkjet printing (IJP) and aerosol jet printing (AJP) seems to fit well in such a kind of context. IJP is a digital non-contact writing technique using liquid materials in small droplets deposited onto the substrate according to a computer-aided design (CAD) file. There are three distinct IJP technologies: continuous, thermal drop-on-demand (DOD), and piezoelectric DOD inkjet printing. In the piezoelectric DOD inkjet, the most used IJP method for PE, a piezoelectric actuator generates the pressure pulse in the fluid to force out the droplets from the nozzle [20–22]. Compared to other technologies, IJP can be used in different configurations from desktop printers to high precision systems that use multiple nozzles simultaneously in combination with techniques for printing support material for PCB prototyping. For example, Nano Dimension developed a system based on an inkjet printer and optimized 3D software to print electronic circuits [23]. AJP is a material jetting additive manufacturing technique, consisting of an aerodynamic focusing process of liquid particles (without using masks) that are accurately deposited onto different kinds of substrates placed under the exit nozzle. AJP overcomes some typical IJP defects, such as nozzles clogging, the coffee-ring effect of droplets, limited inks viscosity range. Unlike most printed technologies (included IJP), AJP can

also print on non-planar substrates and 3D complex surfaces, allowing (1) the realization of custom sensors and electronics on any kind of surface in a controlled manner [24,25], (2) the fast fabrication of smart devices on ready-to-use objects, and (3) easier wiring and interconnections between circuits, avoiding the use of wires and glue [26,27].

In light of this, the aim of this work is to analyze the opportunities of PE, specifically, IJP and AJP also combined with flash lamp annealing (FLA). FLA, known also as photonic curing, uses xenon flash lamps to generate a light pulse that radiates energy toward the sample, especially the ink for the curing [28]. The curing process is essential to remove solvents and other additives and to obtain the best performance of the printed ink (adhesion, electrical properties, etc.). Unlike traditional oven processing, FLA is a promising technique to heat to high temperature thin films deposited on low-melting-point substrates (such as some plastics, fabrics, paper-based materials, etc.) without damage. Section 2 will define typical architectures for smart objects, Section 3 will present some sensors (piezoelectric sensors, strain gauges, and temperature sensors) developed through the above-mentioned technologies, while Section 4 will discuss the technologies making a comparison and defining possible future perspectives.

2. Smart Object Architectures

An everyday object that embeds sensors, electronics, and net protocols could be transformed into a smart object [29]. For example, a gas knob was transformed into a smart object with the additional functions of detecting the motion of the knob (on-off) and transmitting these data to a server via the WiFi module [30]. A smart object is an object that preserves the function for which it was created, and it can perceive changes in specific physical quantities (temperature, humidity, mechanical deformations, etc.) through its sensors and to elaborate information starting from sensor measurements. The elaborated information can be used by the smart object to make decisions autonomously or can be sent to other objects, devices, or users [3]. The shared data can be delivered to the cloud server, and data mining and machine learning algorithms can exploit this information to performing diagnosis, optimize and reconfigure intelligent product lines [31,32]. A typical smart object can exchange data wirelessly and no cabled lines (for example, main power supply) are required to supply the electronics, therefore no cables and wires run across the factory/environment to supply or to communicate with the smart object.

According to their architecture, smart objects can be classified into active or passive smart objects. Active smart objects require an internal energy source to supply its electronics, while passive smart objects use passive elements to be interrogated wirelessly by an external readout unit.

A typical block diagram of an active smart object is shown in Figure 1a. It contains:

- Sensor(s): one or more sensing elements react to specific changes.
- Sensor interface: analog and digital circuits read and pre-elaborate the sensor output.

Processing unit: a microcontroller (MCU) or other programmable chip solutions transform the sensor measurement into a piece of digital information ready to be stored or shared over the network. The processing unit can make decisions according to its internal status and the sensor output, it sends or stores information autonomously, as well as it can interact with other objects, devices, and users if a user interface is implemented on the smart object.

- Wireless transceiver: this block includes an antenna and the protocol to communicate with the network through the gateway. The cloud/Internet block connects smart objects, devices, users, machines, and the industrial control system, and allows to access and store data.
- Power Unit: this block includes an internal power supply (battery, energy storage unit, etc.) and the power management unit to store, control, and distribute the electrical power to the electronic parts.

Temperature, Deformation, Vibration, Force, etc.

Sensor (s)

Active Smart Object

Data Sensing and Collection
Processing and Action
Data Exchange and Connectivity

Sensor interface

Processing Unit
MCU/ DSP
Memory

Power Supply Unit
Power Management Unit
Accumulator(s)

Natural Energy (Light, Vibration, Radio Wave, Thermal, etc.)

Wireless Transceiver

Cloud / Internet

Gateway/ Hub

(a)

Temperature, Deformation, Vibration, Force, etc.

Sensor

Passive Smart Object

Data Sensing
Data Exchange

Data Exchange Link

Readout Unit

Sensor Interface and Data Collection
Processing and Action
Data Exchange and Connectivity

Sensor Interface

Processing Unit

Power Supply Unit

Transceiver

Gateway /Hub

Cloud / Internet

Natural Energy (Light, Vibration, Radio Wave, Thermal, etc.)

(b)

Figure 1. Architectures of (**a**) active and (**b**) passive smart objects. The smart object is equipped with sensors that detect changes in physical quantities like temperature, deformation, vibration, etc. In the case of active smart objects, electronics acquires, processes, and exchanges data with the network, while in the case of passive objects, an external readout unit acquires the sensor output wirelessly. The power supply unit can include (1) batteries, accumulator or systems that convert other natural energies into electrical energy and (2) a power management unit that controls and distributes the power supply (orange arrow) to the other blocks.

The processing unit and the power management unit also monitor the internal status (battery level, energy consumption, etc.) of the smart object and they may detect and manage fault conditions [33]. Batteries are the typical power source that supplies sensors and electronics. Battery-powered systems are affected by maintenance issues related to regular battery replacement or charging, as well as by a decrease in rechargeable battery life. Energy harvesting is a valid alternative to the batteries since it can reduce maintenance issues related to the battery replacement, sometimes without compromising the final weight and exploiting wasted energy present in the environment (thermal energy, kinetic energy, solar power, etc.) [34]. Despite the small levels of power in the nW–mW range [35], the power harvesting system can be properly designed to support smart objects, considering that low power consumption is one of the main requirements of smart objects. For example, in [36], a self-powered smartwatch for continuous sweat glucose monitoring was designed to be supported by the harvested/converted solar energy without external charging.

Smart objects can transfer data, communicate with other devices connected to the same network through various protocols/technologies such as cellular technology (GSM/3G/4G) [37], WiFi [38], Bluetooth Low Energy (BLE) [39] and ZigBee [40].

Passive smart objects may represent a viable solution when the measurement elaboration should be demanded externally due to application constraints. The object is equipped with a passive sensor and other passive components, and it requires an external readout unit for the acquisition and the processing of the sensor measurements. The typical block diagram of a passive smart object is depicted in Figure 1b. The smart object measures the changes in a specific physical quantity and the readout unit acquires these measurements and performs other tasks like the active smart object. This particular telemetric system uses passive wireless communication, exploiting an electric-magnetic [41], optic or acoustic link [42]. For example, in [41], the resistance of a temperature sensor was read by using two inductors, one connected to the sensor and the other to the readout unit. The resistance change of the temperature sensor induces a change in the impedance of the inductor of the readout unit. This type of telemetric system does not require any battery or power supply for the passive smart object, which can be placed easily inside a harsh or hermetic environment, but the distance between the two inductors has to be lower than a few centimeters. A telemetric system was successfully adopted for monitoring hermetic or inaccessible environments, such as furnaces [43] or pipes of the heating plant [41]. In the case of the telemetric device, the readout unit also acts as a bridge between the passive device and the factory network.

3. Sensors for Smart Object by Inkjet and Aerosol Jet Printing

In this section, some examples of printed sensors fabricated through IJP and AJP were reported: (1) printed piezoelectric sensors obtained by using AJP were designed for active smart objects; (2) strain sensors fabricated by IJP and AJP were proposed for passive and active smart objects; (3) temperature sensors were fabricated by AJP for active and passive smart objects. The proposed sensors could be used to measure vibrations, mechanical deformation, or temperature that could affect the production process in the industrial field.

3.1. Printed Piezoelectric Sensors for Active Smart Object

Axial and shear load sensors (Figure 2a) were obtained by depositing a piezoelectric layer based on lead-zirconate-titanate (PZT) ink with aerosol jet printing [44]. Figure 2a shows the loading direction for both sensors. The ink was obtained by combining APC 850 PZT powder (30%), deionized water (49.6%), ethylene glycol (12.4%) with two dispersants, DisperBYK-180 (5%) and polyvinylpyrrolidone (3%) to improve the ink adhesion onto the substrate. Alumina substrates were selected since they can withstand high temperatures under the curing process. Figure 2b summarized the fabrication process adopted for axial and shear load sensors, which differ for electrodes geometry. Bottom electrodes were made of conductive silver-palladium paste, deposited by screen printing. The deposited ink was firstly dried at 150 °C for 10 min and then sintered at 950 °C for 30 min. Custom piezoelectric ink was then deposited by AJP. Two consecutive crossed depositions were made for a total of ten passes interspersed with drying in an oven at 200 °C for 2 h, while the final sintering step was realized in an IR oven at 850 °C for 1 h. The printed PZT area was 3 mm × 3 mm. Top electrodes were printed and cured as described for the first electrodes. After the production step, the poling phase was performed at 500 V for 30 min in the oven at 150 °C; then, the oven was switched off and cooled down maintaining the voltage for 40 min. The voltage was applied across the thickness for axial sensors and between the two bottom electrodes for shear sensors, as shown in Figure 2b (on the bottom). d_{33} is of particular significance in axial sensors because it represents the ratio between the induced polarization (parallel to the direction in which PZT element is polarized) per unit stress applied in the same direction; instead, d_{15} is the most relevant one in shear sensors, because it represents the ratio between the induced polarization (perpendicular to the direction in which PZT element is polarized) per unit stress applied in the direction perpendicular to the induced polarization and perpendicular to the direction in which

PZT element was polarized. The two bottom electrodes of the shear sensors were then shorted to increase the area of the bottom electrode. To properly characterize shear sensors, an alumina layer was glued on the top electrode of each shear sensor as shown in Figure 2a (on the bottom). The final devices are shown in Figure 2c.
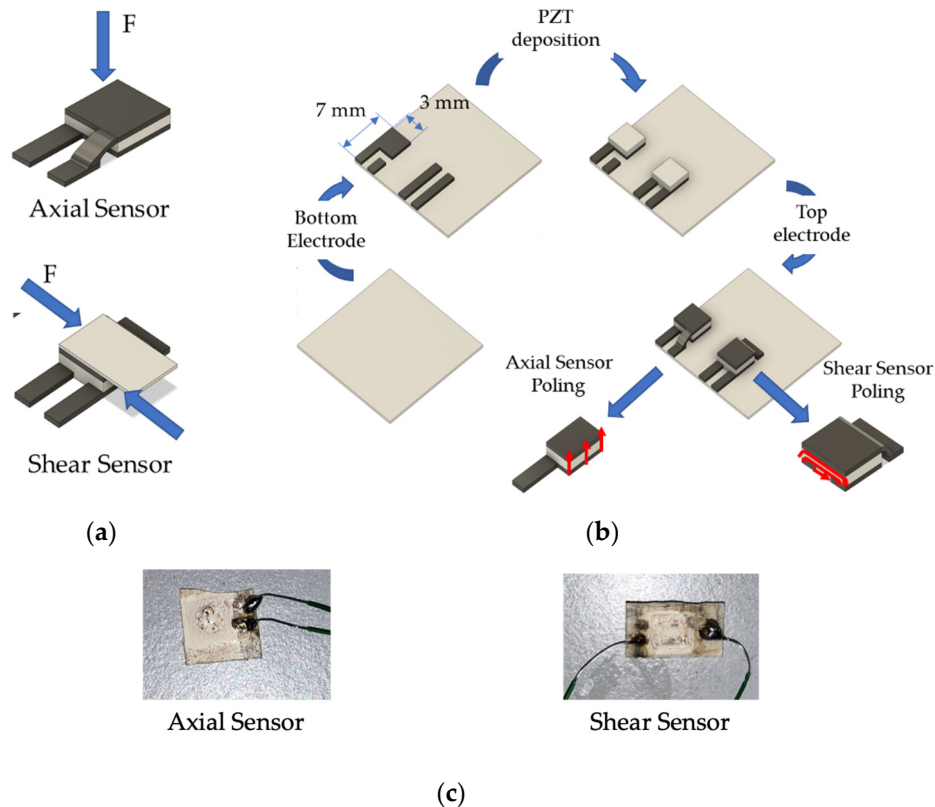

(a)

(b)

(c)

Figure 2. (**a**) Loading direction for axial and shear sensors; (**b**) Block diagram of the production process. (**c**) Axial and shear sensors.

Crosshatch ink adhesion tape test, described in the standard ISO 4624:2016 [45], confirmed the good adhesion of the inks to underlying printed layers and alumina.

The thickness of PZT and the final device measured by an optical profilometer (Profilm3D, Filmetrics) were 100 and 270 μm, respectively.

The piezoelectric coefficients d_{33} and d_{15} were obtained by d_{33} m (YE 2730 A, APC Products) and electrical capacitance (between the bottom and top electrode) by impedance/gain-phase analyzer (HP 4194A, Hewlett Packard). The mean capacitance was calculated by averaging the capacitance of five sensors measured in the range of 100 Hz to 1 MHz. The axial sensors showed a mean capacitance of (14.9 ± 6.0) pF and a mean d_{33} coefficient of (65 ± 21) pC N^{-1}, with a maximum value of 101 pC N^{-1}, far from what declared by the manufacturer of the powder (d_{33} = 400 pC N^{-1}) due to different production processes. Shear sensors showed a mean capacitance of (1.8 ± 0.5) pF and a mean piezoelectric coefficient of (5.5 ± 1.6) pC N^{-1}. The capacitance of the shear sensors is lower than one of the axial sensors due to the different poling method and the geometry of the bottom electrode.

The proposed PZT sensors can be fabricated on active smart objects, if the support materials are compatible with the curing temperature, leveraging the power of AJP.

3.2. Strain Gauge Printed by IJP for Active and Passive Smart Object

A strain gauge was fabricated by depositing a conducting polymer poly(3,4-ethylenedioxythiophene): poly(styrene sulfonate) (PEDOT:PSS) ink on a polyimide foil (25 μm of thickness) by ultralow-cost inkjet printer (Epson XP205). The fabrication method is shown in Figure 3 and it was described in [46].
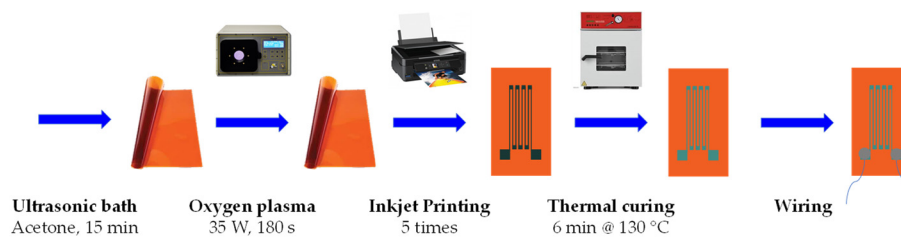
Figure 3. Fabrication process by inkjet printing for poly(3,4-ethylenedioxythiophene):poly(styrene sulfonate) (PEDOT:PSS) -based strain gauge.

PEDOT:PSS strips and tracks fabricated by inkjet printing can be modeled as an ideal resistor, as proved in [46]. PEDOT:PSS is highly conductive, environmentally friendly, biocompatible, and mechanically flexible. Polyimide is often used as a substrate due to the wide range of working temperatures and the stability to environmental factors. Due to the hydrophobic behavior of polyimide, the substrate was cleaned with ethanol and its surface was modified by plasma treatment under the oxygen atmosphere before deposition. The deposition process was repeated five times to reach the desired resistance (68 kΩ). The printed sensor was then dried at 130 °C for 6 min and wires were glued to the electrical contacts with conductive epoxy glue. The final sensor is shown in Figure 4a. Crosshatch ink adhesion tape test confirmed the effectiveness of the plasma treatment for the adhesion of PEDOT:PSS to polyimide.
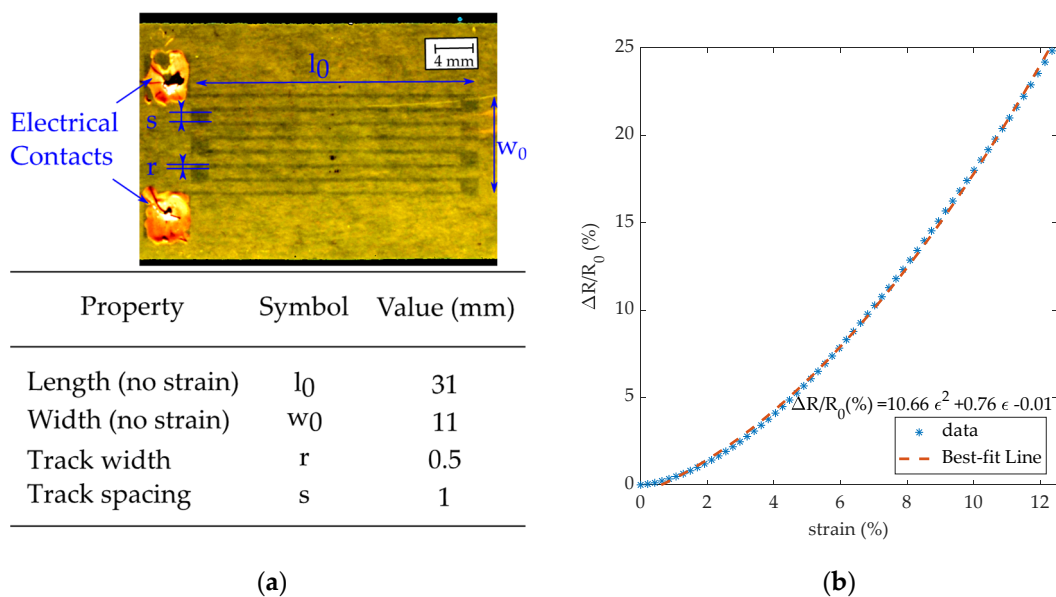

Property	Symbol	Value (mm)
Length (no strain)	l_0	31
Width (no strain)	w_0	11
Track width	r	0.5
Track spacing	s	1

(**a**)

$$\Delta R/R_0 (\%) = 10.66\,\epsilon^2 + 0.76\,\epsilon - 0.01$$

(**b**)

Figure 4. (**a**) Printed strain gauge. (**b**) Strain–resistance curve, where R_0 is the resistance with no strain.

To find the strain–resistance curve of the strain gauge (Figure 4b), both ends of the strain sensor were fixed to an electromechanical dynamometer (Instron, model3366), equipped with a 500 N load cell and screw-type grips. The tensile configuration of the dynamometer induced and measured a uniaxial deformation (parallel to the length direction) of the sensor, and the electrical resistance was measured by HP34401 multimeter using 4-wire configuration. A silver paste (DuPont 5028) was deposited on the sensor pads for the electrical contact between the wires and the sensor. As shown in Figure 4b, the strain-resistance is not linear but could be approximated by a second-order line (dashed, line). With respect to silver-based strain gauges, the sensitivity and the strain limit of the PEDOT:PSS-based sensors are higher due to the electrical and mechanical properties. Indeed, the conduction pathways within each grain occur differently with respect to the nanoparticle silver.

The proposed sensor can be easily used on an active smart object or it can be connected to an inductor and interrogated through the telemetric techniques proposed in [47,48]. For example, in [48], a printed system (strain gauge and inductor) was used to detect the deformation induced in the printed strain sensor, and the deformation was easily derived by measuring the change in phase of the impedance of the passive telemetric system at which the sensor was connected.

3.3. Strain Gauge Printed by AJP for Passive and Active Smart Devices

Strain sensors were also fabricated on 3D plastic surfaces by AJP and FLA. Figure 5 shows schematically the method for fabricating a strain gauge sensor and conductive tracks directly onto a PVC tube. The 2D model of the designed pattern was drawn with CAD design tools and it was used by the AJP software to control the 3D movements of the platen and the printhead. After cleaning the surface with ethanol, the pattern was printed onto the surface fixed to the moving platen by using the AJP technology. The printing process was repeated two times to reach the desired thickness and resistance. Then, the printed device was dried at room temperature for 30 min and it was put inside the FLA machine to sinter the deposited ink. Finally, an epoxy conductive paste was used to create the electrical contact between the printed pad and the wire. The fabrication method was also described in [49].
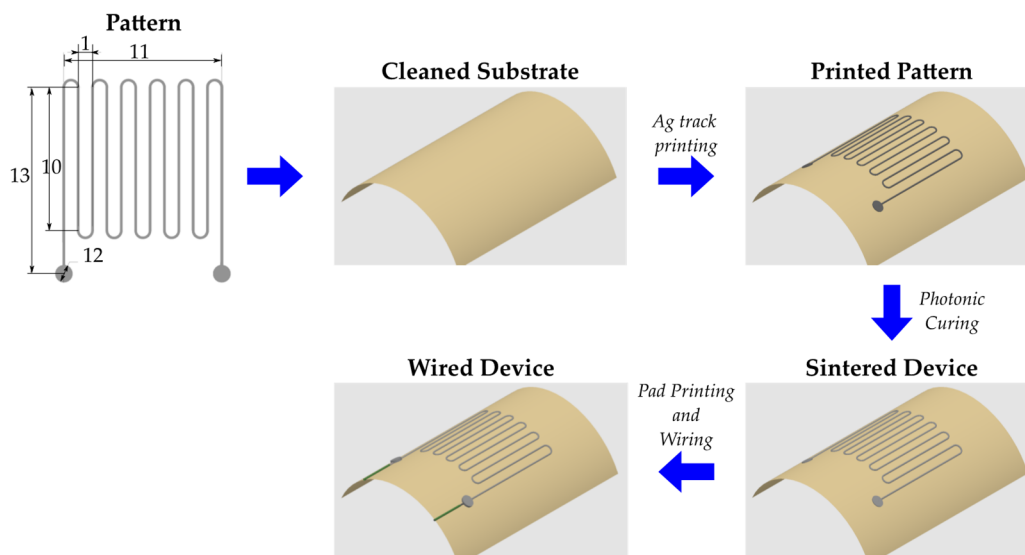

Figure 5. Diagram of the circuit manufacturing steps: (1) Preparation of the 2D model of the printed device with serpentine pattern (in mm); (2) Cleaning of the surface with solvent to remove dust and dirt; (3) Deposition of Ag ink with Aerosol Jet Printing (AJP) according to the 3D model and drying at room temperature; (4) Curing of the resulting device with Flash Lamp Annealing (FLA) (5) Deposition of epoxy conductive paste to fix the wires and create the electrical contacts with the deposited ink.

The method can be adapted to print various patterns (even complex) onto various 3D surfaces, even on surface slopes up to 90 degrees by tilting the nozzle head [50]. To test the fabrication method, a serpentine pattern was fabricated with the proposed method onto different surfaces and plastic materials: polylactic acid (PLA), a typical material used in additive manufacturing to develop prototypes, polypropylene and soft PVC. Figure 6a shows a surface in PLA, a combination of square pyramids (1.5 mm × 1.5 mm × 0.5 mm). The printed serpentine was printed on a lid of 54 mm diameter in polypropylene (Figure 6b) and on a PVC conduit of 20 mm diameter (Figure 6c). The printing process was repeated two times before the curing process. Crosshatch ink adhesion tape test confirmed the adhesion of silver ink to plastics.
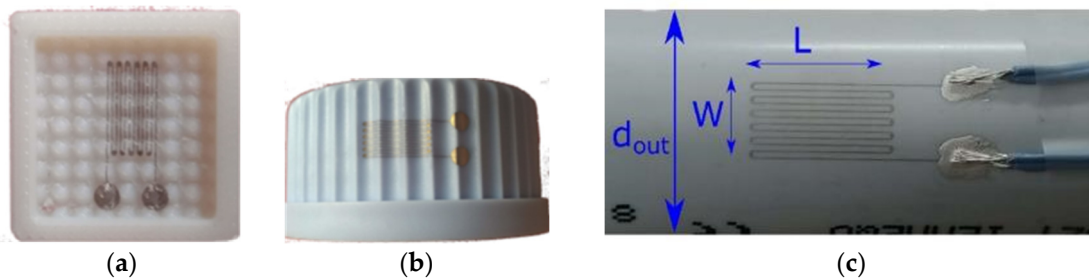
Figure 6. Example of printed serpentine devices with the proposed method. Printed device: (**a**) on different 3D surfaces 2.4 cm × 2.4; (**b**) on a 5.6 cm diameter cap; (**c**) on a PVC conduit of 20 mm diameter (d_{out}). Strain gauge dimensions: active gauge length (L) is 10 mm and the gauge width (W) is 5.5 mm.

Finally, the sensor printed on the 400-mm long PVC tube (Figure 6c) was tested as a strain gauge sensor. The thickness and the width of the printed tracks resulted in 13 μm and 120 μm, respectively, by measuring the profile with the optical profilometer Profilm3D. The output was compared with an off-the-shelf strain gauge (commercialized by RS PRO and 2 mm long) under tensile conditions, and the PVC conduit was used as cantilever beam for the experimental validation (Figure 7a). Different loads were applied to the free end of the conduit to induce different levels of strain (from 0 to 0.25%). The strain was measured by a digital image correlation (DIC) system (Aramis Adjustable), while the electrical resistance of the sensor was monitored by a multimeter (HP34401A). The commercial sensor was glued to the conduit in the same position and it was tested with the same method. The strain–resistance curve of both sensors could be considered linear (Figure 7b). The resulting gauge factor of the commercial sensor and of the printed sensor was 2.12 and 2.55, respectively.
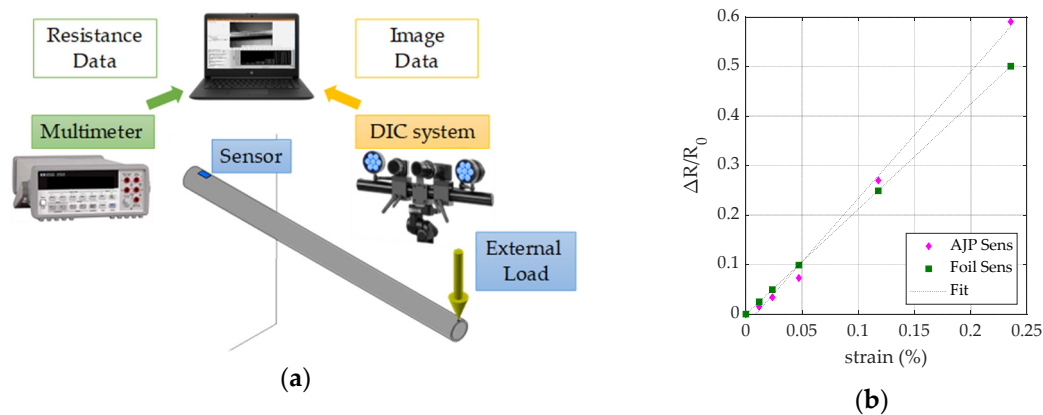

Figure 7. (**a**) Experimental setup for tested the response of the printed strain gauge under axial stress and (**b**) experimental results compared with the ones of the commercial strain gauge.

The sensor was tested also inside a climatic chamber (Perani UC 150/70). The thermal coefficient resistance (TCR) was found 150 ppm/°C in the temperature range of 0 to 40 °C (humidity 15 ± 2%). The resulted TCR is half of the TCR of the silver bulk.

As concluded for the IJP strain gauge, the AJP strain sensor can be adopted for active and passive smart objects.

3.4. Resistance Temperature Detector Printed by AJP for Active and Passive Smart Devices

Some Resistance Temperature Detectors (RTDs) were aerosol jet printed on polyimide foils (25 μm thick) using a silver nanoparticles ink (UTDAgPA, UTdots, 2716 W. Clark Rd., Suite E. Champaign, IL, USA) in three different length configurations (33, 66, 99 mm), as shown in Figure 8. A pneumatic atomizer was the selected system, together with a 200 μm exit nozzle.

Two consecutive depositions were performed to realize these sensors, followed by an oven sintering at 200 °C for 10 min. Crosshatch ink adhesion tape test confirmed the adhesion of silver ink to polyimide.
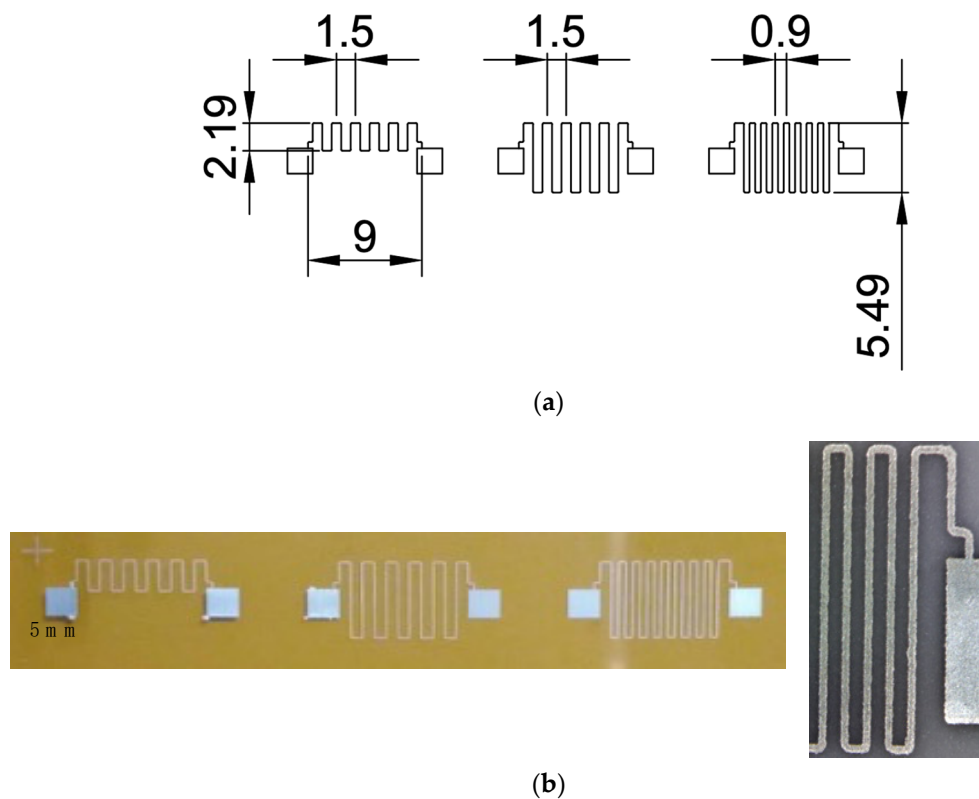

(**a**)

(**b**)

Figure 8. (**a**) 2D model and dimensions (in mm) of printed resistance temperature detector (RTD) and (**b**) printed RTD in three different configurations (33, 66, 99 mm in length) printed on Kapton.

To test the stability of the sensors up to 400 °C, the sensors were spray-coated with a specific protecting layer able to resist until 450 °C, followed by the deposition of a conductive paste applied on pads for electrical contact with wires. Three consecutive thermal cycles at 400 °C for 30 min were performed. The electrical resistance was measured right after the sintering process and after each thermal treatment. Mean resistance values after the sintering process were about (17 ± 2) Ω for the 33-mm long sensor, (40 ± 5) Ω for the 66-mm long sensor, and (60 ± 6) Ω for the 99-mm long sensor. The resistance value measured after the thermal cycles decreased by 40% on average to that after the printing process.

The sensors were then characterized in a controlled temperature oven, using as reference a Pt100 thermo-resistance. This test was performed to define the temperature coefficient α of the sensors in the range 35–140 °C. The results of eight 66-mm long sensors are summarized in Figure 9, where the dots represent the mean value of the printed sensors. The overall α coefficient was obtained from the slope of the best fit straight line (red line) and it is 0.00315 K^{-1}, slightly lower than the α coefficient of bulk silver (α = 0.00380 K^{-1}). The yellow line is the relationship between the output of the reference Pt100 sensor (α = 0.00385 K^{-1}) and the temperature inside the chamber.
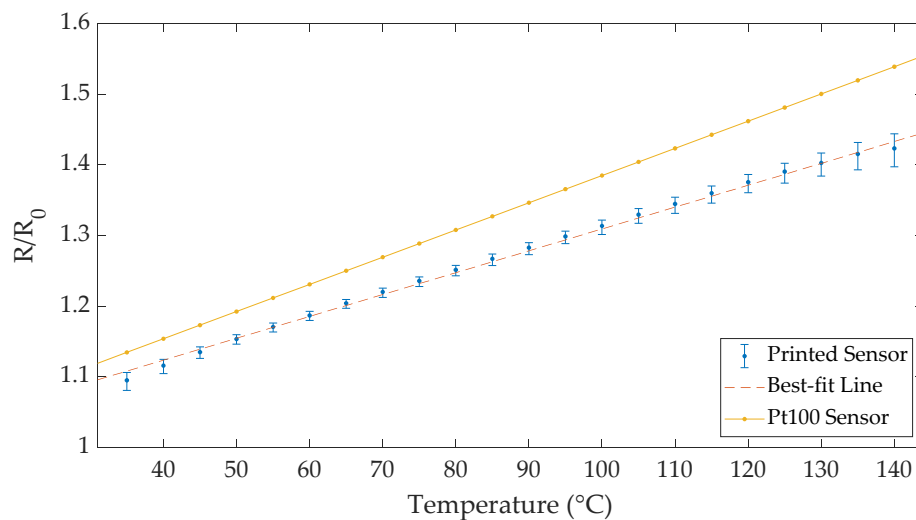
Figure 9. Normalized resistance vs. temperature of the silver sensor (66 mm long) and Pt100 sensor. R_0 is the resistance at 0 °C. Error bars correspond to the output range of eight different sensors.

These resistive sensors can be used in a new dedicated telemetric system for passive smart devices, following the procedure described above for the strain gauge, but with particular attention to the resistance values and the final application [41]. Alternatively, such temperature sensors could be coupled with devoted electronics, microprocessor, and antenna for realizing active smart devices.

4. Discussion

In this work, two specific technologies were proposed to fabricate sensors that can be used for smart objects in the I4.0 context: inkjet printing and aerosol jet printing. Two main architectures of smart objects were analyzed: passive smart objects and active smart objects. Passive smart objects could be fully fabricated through PE technologies. In active smart objects, sensors, antenna, and interconnections could be fabricated by PE, while active components such as microprocessors, integrated circuits (IC) for power management and data transmission should be placed later. Hybrid technologies could be proposed to integrate printing methods with IC components placing on the circuit as proved in [51].

In this work, different examples of sensors for smart objects were proposed. Printed strain gauges, temperature sensors, and piezoelectric sensors were fabricated by using different substrates and inks to prove the flexibility of PE in sensor design and fabrication directly onto the objects. The characterization tests of the proposed sensors showed: (1) the sensitivity (α coefficient) of printed temperature sensors is equal to 0.00315 K^{-1}, and it is similar to industrial Pt100 sensors sensitivity (α = 0.00380 K^{-1}); (2) the printed PEDOT:PSS strain gauges work at higher strain levels (>12%) than commercial foil strain gauges (<4%), and metallic strain gauges have similar performance to commercial foil strain gauges. (3) The variability in the printed process is lower than 13% for resistive sensors made by an ultralow-cost inkjet printer and 6% for AJP resistive sensors. (4) Printed piezoelectric sensors can be fabricated by AJP, but an optimization of the manufacturing process is still required to obtain more sensitive sensors and to improve process variability.

PE offers fabrication methods for sensors and electronic components tailored for the specific application, demonstrating high flexibility in different contexts. For example, AJP and IJP are capable of depositing a large variety of functional materials (organic, metallic, insulating, etc.) to fabricate custom shape sensors onto any surface, even non-planar. In this work, temperature sensors, strain gauges and piezoelectric sensors were fabricated with different shapes and different inks (silver, PEDOT:PSS, and PZT ink). The flexibility of these printing processes was also demonstrated by fabricating different types of strain gauges: in addition to silver-based strain gauges, a strain gauge for high strain levels (>4%) was fabricated by using PEDOT:PSS ink, also considering applications with eco-friendly

requirements. Even a large variety of inks is available, the low solid content of the ink and the low thickness of the printed layers (few micrometers) affect significantly the performance of the final device. For example, in the case of conductive tracks, the resistivity of printed silver tracks was 40 μW cm and this can limit the maximum length of the interconnections of the printed circuit. The viscosity range of the inks suitable for IJP is only 5–20 cP, limiting the use of IJP for PE, while AJP, can deposit inks with higher viscosity (1–1000 cP). Furthermore, lower viscosity ink implies lower solid content and therefore lower thickness of the printed tracks. For example, in the case of the piezoelectric sensors, several depositions were required to increase the sensitivity of the final device and to prevent damages during poling. IJP can reach printing speed up to 5000 mm/s and a resolution of 30 mm, while AJP is a slower process (up to 200 mm/s) but it can reach a resolution of 10 mm [52].

Another important aspect that should be considered is the compatibility of the printing and curing processes with the characteristic of the objects, such as dimensions and materials. For example, IJP is not suitable for 3D surfaces. Another example regards piezoelectric sensors: the object has to be made of a material compatible with the curing step at high temperatures (>800 °C) for a long time (>1 h) and with the poling process at a high DC electric field. For objects made of low-temperature substrates (plastics, fabrics, paper-based materials, etc.), the curing process can be shortened and confined to the deposited ink by using other techniques, such as FLA. For example, in this work, FLA was adopted to sinter silver-based strain gauges printed directly on plastic surfaces. With respect to a traditional oven, in FLA technology, light interacts with few superficial layers and with the deposited ink limiting the damage on the substrate. FLA can cure only a thin printed layer since only the surface of the printed element reaches the modeled temperature, and for this reason, FLA can be adopted for tracks printed through IJP and AJP.

In the future, increasing demand for massive smart objects into smart factories for providing more information on production lines and industrial processes is expected. Both IJP and AJP are promising PE methods for the fabrication of smart objects because these technologies could be integrated into the production line, combining the benefits of mass production and customization; for example, IJP and AJP are currently used to fabricate organic light–emitting diodes (OLEDs) and antennas for smartphones [53,54]. IJP can be scaled to simultaneous and parallel production since more printheads can be easily added; instead, AJP uses only one printhead and a reduced effective working area, limiting the device size and production volume. These limitations can be partially avoided by customizing the AJP printer adding more parallel heads and by implementing a printhead on robotic arms for process optimization. FLA is compatible with mass production, and it can speed up both prototyping and production steps being a rapid process. However, in mass production, reproducibility of subsequent flashes and drifts during long-time operation due to homogeneity of lighting should be considered [55–57].

5. Conclusions

The increasing need for connectivity in many different industrial contexts requires to make objects "smart" through new fabrication methods. A smart object represents a key element for I4.0 because it is able to sense changes in the environment, measuring physical quantities through its sensors, and to share acquired data wirelessly with other smart objects and with industrial management systems, preserving its functionality as an object. The possibility to make tools smart would help to improve the efficiency of factories. Specific technologies for embedding sensors on objects are mandatory.

In this work, smart objects were classified into active and passive smart objects, obtained by IJP and AJP. The main advantage of these technologies is the customization thanks to the flexibility of the printing process in the design and the selection of the inks. Temperature sensors, strain gauges, and piezoelectric sensors were fabricated to test the feasibility of common sensors to be integrated into smart objects.

Future developments will focus on the metrological performances of the sensors under different conditions (operating temperature and humidity range, stress conditions, etc.) and on the compatibility of the fabrication process with the objects (shape of the surface, materials requirements, etc.).

Inkjet printing and aerosol jet printing demonstrated to be promising technologies for making traditional objects smart. PE could offer low-cost and affordable manufacturing processes. Further research activity on the more recent PE technologies is still required to reach large-scale smart object production.

Author Contributions: Data curation, M.B. and E.C.; Investigation, M.B. and E.C.; Supervision, E.S. and M.S.; Validation, M.B. and E.C.; Writing—original draft, M.B. and E.C.; Writing—review & editing, M.B., E.C., E.S. and M.S. All authors have read and agreed to the published version of the manuscript.

Conflicts of Interest: The authors declare no conflict of interest.

References

1. Traini, E.; Bruno, G.; D'Antonio, G.; Lombardi, F. Machine Learning Framework for Predictive Maintenance in Milling. *IFAC-PapersOnLine* **2019**, *52*, 177–182. [CrossRef]
2. Bin Iqbal, M.I.; Mohsin, M.; Gula, F. Smart-Genie: An IoT-enabled Predictive Health Monitoring System for Power Generators. In Proceedings of the 2019 15th International Conference on Emerging Technologies (ICET), Peshawar, Pakistan, 2–3 December 2019.
3. Kortuem, G.; Kawsar, F.; Sundramoorthy, V.; Fitton, D. Smart objects as building blocks for the Internet of things. *IEEE Internet Comput.* **2009**, *14*, 44–51. [CrossRef]
4. Munirathinam, S. Industry 4.0: Industrial Internet of Things (IIOT). *Adv. Comput.* **2020**, *117*, 129–164. [CrossRef]
5. Gokalp, M.O.; Kayabay, K.; Akyol, M.A.; Eren, P.E.; Koçyiğit, A. Big Data for Industry 4.0: A Conceptual Framework. In Proceedings of the 2016 International Conference on Computational Science and Computational Intelligence (CSCI), Las Vegas, NV, USA, 15–17 December 2016; pp. 431–434.
6. Ruppert, T.; Jaskó, S.; Holczinger, T.; Abonyi, J. Enabling Technologies for Operator 4.0: A Survey. *Appl. Sci.* **2018**, *8*, 1650. [CrossRef]
7. Özbek, O.; Saruhan, H. The effect of vibration and cutting zonetemperature on surface roughness and tool wear ineco-friendly MQL turning of AISI D2. *J. Mater. Res. Technol.* **2020**, *9*, 1–11. [CrossRef]
8. Cohen, Y.; Faccio, M.; Pilati, F.; Yao, X. Design and management of digital manufacturing and assembly systems in the Industry 4.0 era. *Int. J. Adv. Manuf. Technol.* **2019**, *105*, 3565–3577. [CrossRef]
9. Eldemerdash, T.; Abdulla, R.; Jayapal, V.; Nataraj, C.; Abbas, M.K. Iot Based Smart Helmet for Mining Industry Application. *Int. J. Adv. Sci. Technol.* **2020**, *29*, 373–387.
10. Jiménez, M.A.; Irigoien, I.; Boto, F.; Sierra, B.; Rodriguez, G. Predictive Maintenance on the Machining Process and Machine Tool. *Appl. Sci.* **2019**, *10*, 224. [CrossRef]
11. Perez-Alfaro, I.; Gil-Hernandez, D.; Munoz, O.; Casbas-Gimenez, J.; Sánchez, J.C.; Murillo, N. Low-Cost Piezoelectric Sensors for Time Domain Load Monitoring of Metallic Structures During Operational and Maintenance Processes. *Sensors* **2020**, *20*, 1471. [CrossRef]
12. Antomarioni, S.; Pisacane, O.; Potena, D.; Bevilacqua, M.; Ciarapica, F.E.; Diamantini, C. A predictive association rule-based maintenance policy to minimize the probability of breakages: Application to an oil refinery. *Int. J. Adv. Manuf. Technol.* **2019**, *105*, 3661–3675. [CrossRef]
13. Fernandes, M.; Canito, A.; Corchado, J.M.; Marreiros, G. Fault Detection Mechanism of a Predictive Maintenance System Based on Autoregressive Integrated Moving Average Models. In *Distributed Computing and Artificial Intelligence, 15th International Conference*; Springer Science and Business Media LLC: Berlin, Germany, 2019; Volume 1003, pp. 171–180.
14. Ruiz-Sarmiento, J.; Monroy, J.; Moreno, F.-A.; Galindo, C.; Bonelo, J.-M.; Gonzalez-Jimenez, J. A predictive model for the maintenance of industrial machinery in the context of industry 4.0. *Eng. Appl. Artif. Intell.* **2020**, *87*, 103289. [CrossRef]
15. Zymelka, D.; Togashi, K.; Kobayashi, T. Concentric Array of Printed Strain Sensors for Structural Health Monitoring. *Sensors* **2020**, *20*, 1997. [CrossRef] [PubMed]

16. Almuslem, A.; Shaikh, S.F.; Hussain, M.M. Flexible and Stretchable Electronics for Harsh-Environmental Applications. *Adv. Mater. Technol.* **2019**, *4*, 1900145. [CrossRef]

17. Gu, Y.; Park, D.; Gonya, S.; Jendrisak, J.; Das, S.; Hines, D.R. Direct-write printed broadband inductors. *Addit. Manuf.* **2019**, *30*, 100843. [CrossRef]

18. Stringer, J.; Althagathi, T.M.; Tse, C.C.; Ta, V.D.; Shephard, J.D.; Esenturk, E.; Connaughton, C.; Wasley, T.J.; Li, J.; Kay, R.W.; et al. Integration of additive manufacturing and inkjet printed electronics: A potential route to parts with embedded multifunctionality. *Manuf. Rev.* **2016**, *3*, 12. [CrossRef]

19. Horst, D.; Duvoisin, C.; Vieira, R. Additive Manufacturing at Industry 4.0: A Review. *Int. J. Eng. Tech. Res.* **2018**, *8*, 3–8.

20. Al-Halhouli, A.T.; Qitouqa, H.; Alashqar, A.; Abu-Khalaf, J. Inkjet printing for the fabrication of the flexible/stretchable wearable electronic devices and sensors. *Sens. Rev.* **2018**, *38*, 438–452. [CrossRef]

21. Prudenziati, M.; Hormadaly, J. Technologies for printed films. *Print. Films* **2012**, 3–29. [CrossRef]

22. Khan, S.; Lorenzelli, L.; Dahiya, R.S. Technologies for Printing Sensors and Electronics Over Large Flexible Substrates: A Review. *IEEE Sensors J.* **2014**, *15*, 3164–3185. [CrossRef]

23. Nano Dimension. Available online: https://www.nano-di.com/ (accessed on 21 October 2020).

24. C, A.; Szymanski, M.Z.; Luszczynska, B.; Ulański, J. Inkjet Printing of Super Yellow: Ink Formulation, Film Optimization, OLEDs Fabrication, and Transient Electroluminescence. *Sci. Rep.* **2019**, *9*, 8493. [CrossRef]

25. Hong, K.; Kim, S.H.; Mahajan, A.; Frisbie, C.D. Aerosol Jet Printed p- and n-type Electrolyte-Gated Transistors with a Variety of Electrode Materials: Exploring Practical Routes to Printed Electronics. *ACS Appl. Mater. Interfaces* **2014**, *6*, 18704–18711. [CrossRef] [PubMed]

26. Clifford, B.; Beynon, D.; Phillips, C.; Deganello, D. Printed-Sensor-on-Chip devices—Aerosol jet deposition of thin film relative humidity sensors onto packaged integrated circuits. *Sens. Actuators B Chem.* **2018**, *255*, 1031–1038. [CrossRef]

27. Tan, H.-W.; Tran, T.; Chua, C.K. A review of printed passive electronic components through fully additive manufacturing methods. *Virtual Phys. Prototyp.* **2016**, *11*, 271–288. [CrossRef]

28. Das, S.; Cormier, D.; Williams, S. Potential for Multi-functional Additive Manufacturing Using Pulsed Photonic Sintering. *Procedia Manuf.* **2015**, *1*, 366–377. [CrossRef]

29. Silverio-Fernandez, M.A.; Renukappa, S.; Suresh, S. What is a smart device?—A conceptualisation within the paradigm of the internet of things. *Vis. Eng.* **2018**, *6*, 3. [CrossRef]

30. Garg, S.; Chatterjee, J.M.; KumarAgrawal, R. Design of a Simple Gas Knob: An Application of IoT. In Proceedings of the 2018 International Conference on Research in Intelligent and Computing in Engineering (RICE), San Salvador, El Salvador, 22–24 August 2018; pp. 1–3.

31. Saqlain, M.; Piao, M.; Shim, Y.; Lee, J.Y. Framework of an IoT-based Industrial Data Management for Smart Manufacturing. *J. Sens. Actuator Netw.* **2019**, *8*, 25. [CrossRef]

32. Xu, X.; Hua, Q. Industrial Big Data Analysis in Smart Factory: Current Status and Research Strategies. *IEEE Access* **2017**, *5*, 17543–17551. [CrossRef]

33. Tsenempis, I.; Filios, G.; Katsidimas, I.; Nikoletseas, S. Energy Harvesting and Smart Management Platform for Low Power IoT Systems. In Proceedings of the 2019 15th International Conference on Distributed Computing in Sensor Systems (DCOSS), Santorini Island, Greece, 29–31 May 2019; pp. 339–346.

34. Pop-Vadean, A.; Pop, P.P.; Latinovic, T.; Barz, C.; Lung, C. Harvesting energy an sustainable power source, replace batteries for powering WSN and devices on the IoT. *IOP Conf. Series Mater. Sci. Eng.* **2017**, *200*, 12043. [CrossRef]

35. Soin, N. Chapter 10—Magnetic Nanoparticles—Piezoelectric Polymer Nanocomposites for Energy Harvesting. In *Micro and Nano Technologies*; El-Gendy, A.A., Barandiarán, J.M., Hadimani, R.L.B.T.-M.N.M., Eds.; Elsevier: Amsterdam, The Netherlands, 2018; pp. 295–322.

36. Zhao, J.; Lin, Y.; Wu, J.; Nyein, H.Y.Y.; Bariya, M.; Tai, L.-C.; Chao, M.; Ji, W.; Zhang, G.; Fan, Z.; et al. A Fully Integrated and Self-Powered Smartwatch for Continuous Sweat Glucose Monitoring. *ACS Sens.* **2019**, *4*, 1925–1933. [CrossRef]

37. Deroussi, A.; Madi, A.A.; Addaim, A.; Erraoui, A. New Scalable Smart Telemetry for Industrial Systems: IoT solutions. In Proceedings of the 2018 International Conference on Electronics, Control, Optimization and Computer Science (ICECOCS), Kenitra, Morocco, 5–6 December 2018; pp. 1–4.

38. Lou, R.; Hallinan, K.P.; Hallinan, K.P.; Reissman, T. Smart Wifi Thermostat-Enabled Thermal Comfort Control in Residences. *Sustainability* **2020**, *12*, 1919. [CrossRef]

39. Bellitti, P.; Bodini, A.; Borghetti, M.; Filippini, M.; Latronico, N.; Sardini, E.; Serpelloni, M.; Tonello, S. A compact low-power wireless system for in vivo evaluation of heat and moisture exchanger performance. *Meas. Sci. Technol.* **2018**, *30*, 025701. [CrossRef]

40. Del-Valle-Soto, C.; Valdivia, L.J.; Velázquez, R.; Rizo-Dominguez, L.; López-Pimentel, J.C. Smart Campus: An Experimental Performance Comparison of Collaborative and Cooperative Schemes for Wireless Sensor Network. *Energies* **2019**, *12*, 3135. [CrossRef]

41. Bona, M.; Borghetti, M.; Sardini, E.; Serpelloni, M. Telemetric Technique for Passive Resistive Sensors Based on Impedance Real Part Measurement at Fixed Frequency. *IEEE Trans. Instrum. Meas.* **2018**, *67*, 2160–2168. [CrossRef]

42. Fan, Y.; Liu, Y.; Xiao, Q.; Ma, X.; Ji, X.; Sun, P. A passive wireless surface acoustic wave sensor for pillar load measurement. *AIP Adv.* **2019**, *9*, 105305. [CrossRef]

43. Yan, D.; Yang, Y.; Hong, Y.; Liang, T.; Yao, Z.; Chen, X.; Xiong, J. Low-Cost Wireless Temperature Measurement: Design, Manufacture, and Testing of a PCB-Based Wireless Passive Temperature Sensor. *Sensors* **2018**, *18*, 532. [CrossRef]

44. Fapanni, T.; Borghetti, M.; Sardini, E.; Serpelloni, M. Novel Piezoelectric Sensor by Aerosol Jet Printing in Industry 4.0. In Proceedings of the 2020 IEEE International Workshop on Metrology for Industry 4.0 & IoT, Roma, Italy, 3–5 June 2020; pp. 379–383.

45. EN ISO 4624 International Organization for Standardization. *Paints and Varnishes—Pull-o Test for Adhesion*; BeuthVerlag: Geneva, Switzerland, 2016.

46. Borghetti, M.; Ghittorelli, M.; Sardini, E.; Serpelloni, M.; Torricelli, F. Electrical Characterization of PEDOT:PSS Strips Deposited by Inkjet Printing on Plastic Foil for Sensor Manufacturing. *IEEE Trans. Instrum. Meas.* **2016**, *65*, 1–8. [CrossRef]

47. Xie, M.-Z.; Wang, L.-F.; Dong, L.; Deng, W.-J.; Huang, Q.-A. Low Cost Paper-Based LC Wireless Humidity Sensors and Distance-Insensitive Readout System. *IEEE Sensors J.* **2019**, *19*, 4717–4725. [CrossRef]

48. Bona, M.; Serpelloni, M.; Sardini, E.; Lombardo, C.O.; Ando, B. Telemetric Technique for Wireless Strain Measurement From an Inkjet-Printed Resistive Sensor. *IEEE Trans. Instrum. Meas.* **2017**, *66*, 583–591. [CrossRef]

49. Borghetti, M.; Serpelloni, M.; Sardini, E. Printed Strain Gauge on 3D and Low-Melting Point Plastic Surface by Aerosol Jet Printing and Photonic Curing. *Sensors* **2019**, *19*, 4220. [CrossRef]

50. Wilkinson, N.J.; Smith, M.A.A.; Kay, R.W.; Harris, R.A. A review of aerosol jet printing—A non-traditional hybrid process for micro-manufacturing. *Int. J. Adv. Manuf. Technol.* **2019**, *105*, 4599–4619. [CrossRef]

51. Serpelloni, M.; Cantù, E.; Borghetti, M.; Sardini, E. Printed Smart Devices on Cellulose-Based Materials by means of Aerosol-Jet Printing and Photonic Curing. *Sensors* **2020**, *20*, 841. [CrossRef] [PubMed]

52. Zhang, H.; Moon, S.K.; Ngo, T.H. 3D Printed Electronics of Non-contact Ink Writing Techniques: Status and Promise. *Int. J. Precis. Eng. Manuf. Technol.* **2019**, *7*, 511–524. [CrossRef]

53. Kateeva. *The Benefits of Inkjet Printing*; Kateeva: Newark, CA, USA, 2020.

54. Optomec. *Aerosol Jet Printed Antennas*; Optomec: Albuquerque, NM, USA, 2020.

55. Park, B.-G.; Lee, C.-J.; Jung, S.-B. Enhancing adhesion strength of photonic sintered screen-printed Ag circuit by atmospheric pressure plasma. *Microelectron. Eng.* **2018**, *202*, 37–41. [CrossRef]

56. Zhong, Z.; Lee, S.-H.; Ko, P.; Kwon, S.; Youn, H.; Seok, J.Y.; Woo, K. Control of thermal deformation with photonic sintering of ultrathin nanowire transparent electrodes. *Nanoscale* **2020**, *12*, 2366. [CrossRef] [PubMed]

57. Rebohle, L.; Prucnal, S.; Skorupa, W. A review of thermal processing in the subsecond range: Semiconductors and beyond. *Semicond. Sci. Technol.* **2016**, *31*, 103001. [CrossRef]

Publisher's Note: MDPI stays neutral with regard to jurisdictional claims in published maps and institutional affiliations.